Journal of Power Sources 242 (2013) 566–574

Contents lists available at SciVerse ScienceDirect

Journal of Power Sources

journal homepage: www.elsevier.com/locate/jpowsour

Durability evaluation of reversible solid oxide cells

Xiaoyu Zhang [a], James E. O'Brien [a,*], Robert C. O'Brien [b], Gregory K. Housley [a]

[a] Idaho National Laboratory, 2525 N. Fremont Ave., MS 3870, Idaho Falls, ID 83401, USA
[b] Center for Space Nuclear Research, Idaho Falls, ID 83401, USA

HIGHLIGHTS

- Durability evaluation of solid oxide cells in the reversible mode.
- SOFC is not suitable for electrolysis operation directly, while SOEC has an acceptable performance in fuel cell operation.
- One Ceramatec SOEC showed performance improvement during long-term electrolysis operation.

ARTICLE INFO

Article history:
Received 29 October 2012
Received in revised form
22 May 2013
Accepted 25 May 2013
Available online 5 June 2013

Keywords:
Solid oxide cells
High temperature electrolysis
Fuel cell
Durability

ABSTRACT

An experimental investigation on the performance and durability of single solid oxide cells (SOCs) is under way at the Idaho National Laboratory. Reversible operation of SOCs includes electricity generation in the fuel cell mode and hydrogen generation in the electrolysis mode. Degradation is a more significant issue when operating SOCs in the electrolysis mode. In order to understand and mitigate the degradation issues in high temperature electrolysis, single SOCs with different configurations from several manufacturers have been evaluated for initial performance and long-term durability. Cells were obtained from four industrial partners. Cells from Ceramatec Inc. and Materials and Systems Research Inc. (MSRI) showed improved durability in electrolysis mode compared to previous stack tests. Cells from Saint Gobain Advanced Materials Inc. (St. Gobain) and SOFCPower Inc. demonstrated stable performance in the fuel cell mode, but rapid degradation in the electrolysis mode, especially at high current density. Electrolyte–electrode delamination was found to have a significant impact on degradation in some cases. Enhanced bonding between electrolyte and electrode and modification of the electrode microstructure helped to mitigate degradation. Polarization scans and AC impedance measurements were performed during the tests to characterize cell performance and degradation.

1. Introduction

Large-scale non-fossil hydrogen production is an important technology that impacts the hydrogen economy. Approximately 53 million metric tons of hydrogen were produced in 2010 globally. An annual growth rate of 5.6% was forecast for 2011–2016 [1]. However, most hydrogen production is based on fossil fuels including natural gas, oil, and coal. Non-fossil large-scale hydrogen production methods are gaining increasing interest all over the world. High temperature electrolysis (HTE) is one of the most efficient technologies for the production of carbon-free hydrogen at large scale [2,3]. INL has demonstrated HTE at the multi-kW scale with a hydrogen production rate in excess of 5000 NL h^{-1} [3,4]. However, technical barriers need to be resolved before commercialization of HTE technology. The major issue for HTE is long-term performance degradation of the solid oxide electrolysis cells (SOECs) [5–8].

Besides the demand for large-scale hydrogen production, there is growing interest in reversible solid oxide cells (RSOC) [9–15]. By integrating an RSOC system into a power plant, hydrogen can be produced through high temperature electrolysis at times of low power demand and stored as an energy source. During periods of high power demand, additional electricity can be generated from the stored hydrogen by RSOC operation in the fuel cell mode [16,17]. However, although solid oxide fuel cells (SOFCs) can be directly operated in the electrolysis mode, practically they exhibit much higher degradation rates in the electrolysis mode than in fuel cell mode [18,19]. Therefore, degradation in the electrolysis mode becomes a significant problem for RSOC application.

In our previous SOEC stack tests, air electrode delamination, Cr vapor poisoning, microstructure degradation, and seal leakage

* Corresponding author. Tel.: +1 208 526 9096.
E-mail address: james.obrien@inl.gov (J.E. O'Brien).

0378-7753/$ – see front matter © 2013 Elsevier B.V. All rights reserved.
http://dx.doi.org/10.1016/j.jpowsour.2013.05.134

Nomenclature

ASR	area specific resistance (Ω cm^2)
HTE	high temperature electrolysis
i	current density (A cm^{-2})
INL	Idaho National Laboratory
MSRI	Materials and Systems Research Inc.
P&ID	Piping and instrument diagram
RSOC	reversible solid oxide cell
sccm	standard cubic centimeters per minute
SOC	solid oxide cell
SOEC	solid oxide electrolysis cell
SOFC	solid oxide fuel cell
St. Gobain	Saint Gobain Advanced Materials Inc.
V	cell voltage (V)

were found to significantly affect the durability of the stack [20,21]. The investigation on degradation issues was focused on single cells in this paper. A new experimental apparatus was developed for single cell tests. SOCs obtained from Ceramatec, MSRI, St. Gobain, and SOFCPower were investigated experimentally. Initial performance and long-term durability tests were conducted in both the fuel cell and electrolysis modes of operation.

2. Materials and experimental apparatus

The state-of-the-art SOCs used for this study were provided by Ceramatec Inc., Materials and Systems Research Inc. (MSRI), Saint Gobain Advanced Materials (St. Gobain), and SOFCPower Inc.. The cells provided from Ceramatec were electrolyte-supported button cells with 2.25 cm^2 active area, while the others use electrode-supported square cells, 5 cm $\times$ 5 cm in dimension. Materials used in the Ceramatec cells are ScSZ electrolyte, Ni–Ceria steam/hydrogen electrode, and La–Co–Fe oxide-based perovskite air electrode. MSRI, St. Gobain, and SOFCPower used Ni/YSZ-supported cells with 8YSZ electrolyte. LSCF is used as the air electrode material in MSRI and SOFCPower cells, while in St. Gobain cells both modified LSM and LSCF are used. Ceramatec and MSRI cells were fabricated as SOECs, with the microstructure of the cells specifically optimized for operation in the electrolysis mode. St. Gobain and SOFCPower cells were fabricated as SOFCs, and were optimized for long-term operation in the fuel cell mode.

A newly developed single-cell test fixture was used to test the SOCs from MSRI, St. Gobain, and SOFCPower. An exploded view of the test fixture is shown in Fig. 1. The apparatus is designed for single cell and short stack tests in the reversible mode. In addition, Cr poisoning is minimized during long-term tests. Referring to Fig. 1, a hydrogen/steam mixture is fed from the bottom through a 6.35 mm OD coiled Inconel tube into the inlet hole in the bottom of the Hastelloy-X (HastX) base plate. The flow then passes through a slot at the bottom of the Alumina cell holder. A mica/glass cell gasket is placed between the cell holder and the nickel plate for sealing. The nickel plate works as the current collector for the steam electrode. A corrugated nickel flow field and a nickel felt are used for managing the hydrogen/steam flow and for electric conduction. After passing along the bottom of the cell, the flow exits through another slot and vents out via a 9.53 mm OD inconel tube. The outlet tube is sized larger than the inlet tube to minimize the back pressure on the cell seal.

On the air side of the cell, a gold-plated perforated inconel plate is used as the current collector and air flow distributer. Air is introduced through a tube that is welded to the inconel plate. Air flow is distributed along the air side of the cell through an array of

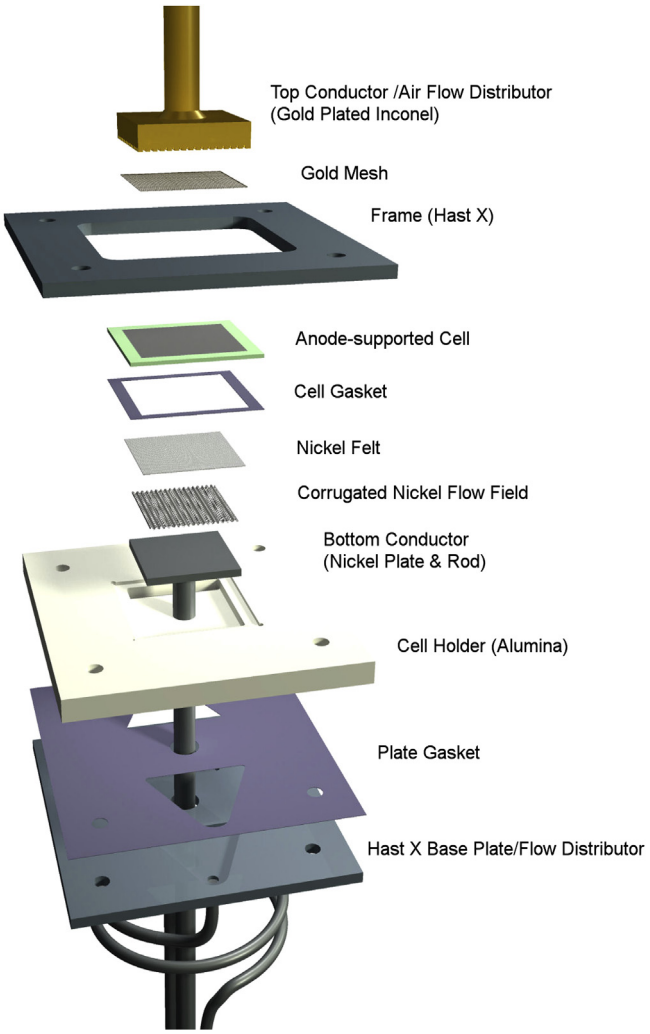

Fig. 1. Exploded view of the cell fixture used for testing MSRI, St. Gobain, and SOFCPower SOCs.

flow channels milled into the bottom of the inconel plate. Air exhaust gas vents out to the furnace. A gold mesh is placed between the air electrode and the plate to minimize ohmic loss and to further improve air flow distribution.

A fixed compression load is applied to the solid oxide cell by means of weights, as shown in the test stand overview, Fig. 2. The load is transferred via an alumina tube from the dead weights to the top cell contact plate. This load simultaneously compresses the cell against the nickel felt, the flow field and the current collector on the bottom steam/hydrogen side of the cell and against the gold mesh on the air side. It also compresses the cell against the seal around the outer edge of the cell which rests on the shelf milled into the alumina cell holder. The HastX weight plates are held in alignment outside of the furnace by the upper portion of the threaded rods which extend upward for this purpose.

The compressive load can also be applied by means of springs. Spring loading is more compact and easier to implement than adding weights. Spring loading was used for the MSRI SOC tests, due to the requirement of incremental loading during the gasket curing process. Weights were used in the St. Gobain and SOFCPower SOC tests.

A photograph of the test stand installed in the furnace base for testing St. Gobain SOCs is shown in Fig. 3. Note that the upper part of the alumina load transfer tube is located outside of the furnace.

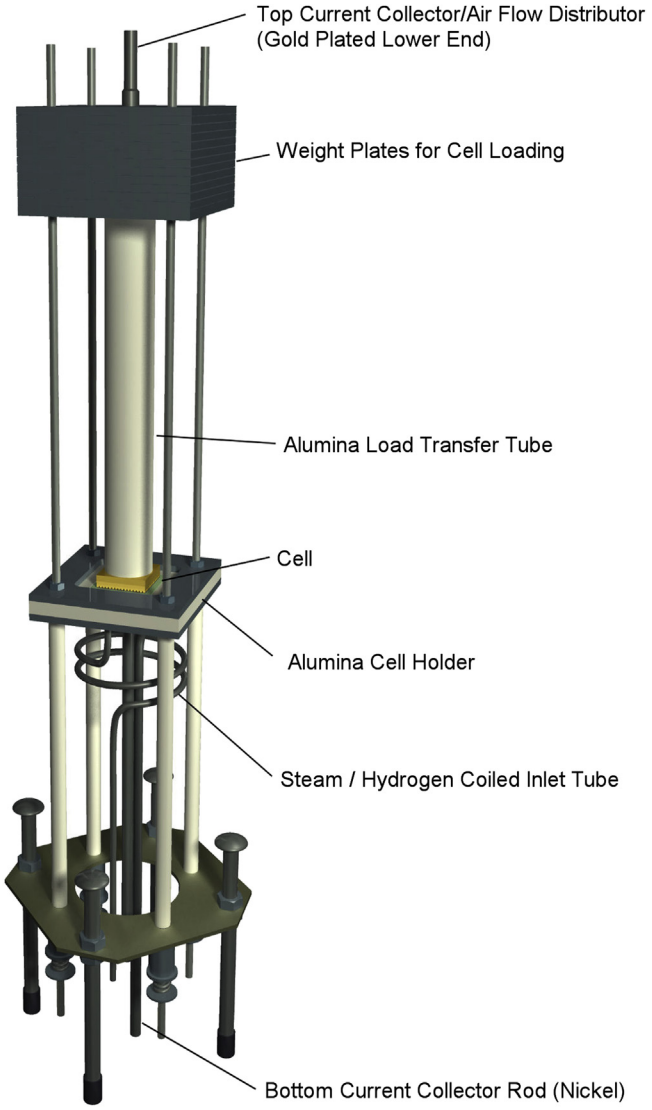

Fig. 2. Test stand overview.

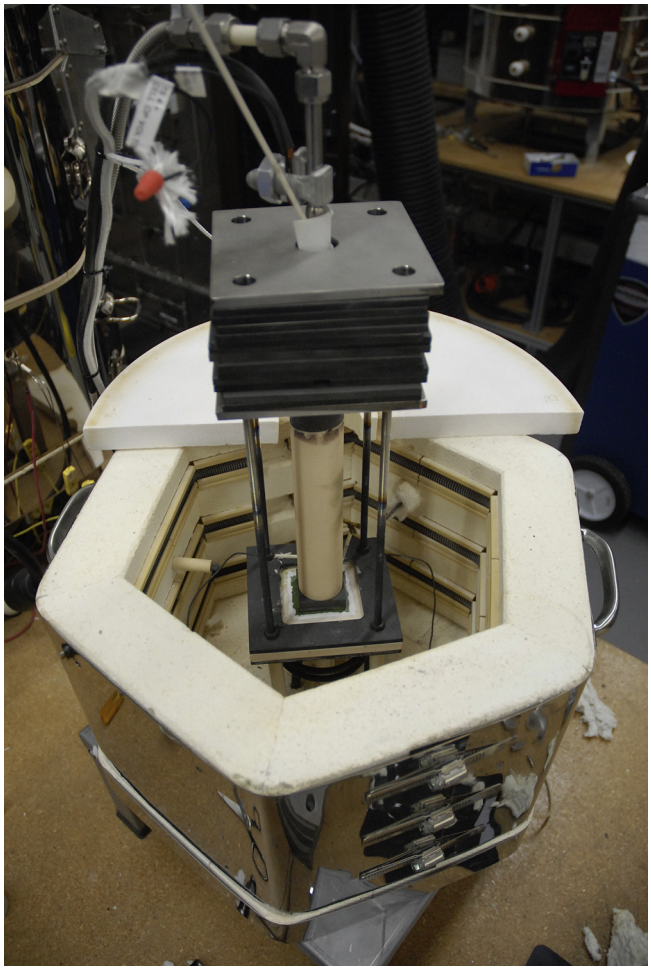

Fig. 3. Single-cell test stand installed in furnace.

So the weights stay outside of the hot zone. Holes were drilled in the bottom of the kiln for pass-through of the flow tubes, the alumina spacer rods, the nickel current collector rod, and instrumentation wires.

The fixture for testing Ceramatec button cells is shown in Fig. 4. The button cell assembly is bonded to one end of an alumina tube using a glass seal. The other end of the alumina tube is fitted with a rubber plug. Two stainless steel tubes penetrate through the rubber plug, providing the gas inlet and outlet flows. The button cell assembly and the lower part of the alumina tube are placed in the hot zone in a cylindrical ceramic fiber furnace.

AC impedance spectroscopy is used to characterize the electrochemical behavior of the SOCs. Impedance measurements were obtained using a Solartron ModuLab 2100A system. Impedance data were obtained in fuel cell mode, electrolysis mode, and at open circuit conditions. During long-term tests, impedance measurements are conducted periodically to characterize the degradation of the cells.

A piping and instrument diagram (P&ID) for the experimental apparatus used for MSRI and St. Gobain single cell testing is presented in Fig. 5. Primary components include gas supply cylinders, mass-flow controllers, a heated water-bath humidifier, online dew

Fig. 4. Button cell test fixture overview.

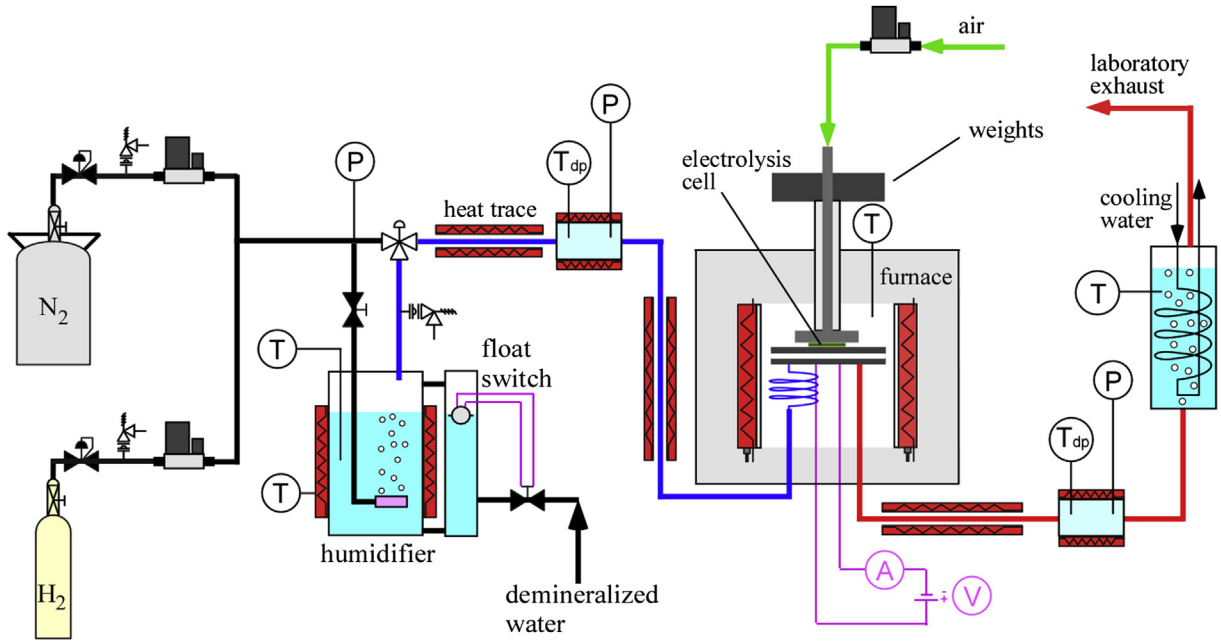

Fig. 5. Piping and instrument diagram for single-cell test apparatus.

point sensors, temperature and pressure measurements, high temperature furnace, and the solid oxide electrolysis cell. Nitrogen is used as an inert carrier gas. Inlet flow rates of nitrogen, hydrogen, and air are established by means of precision mass-flow controllers. Hydrogen is included in the inlet flow as a reducing gas in order to prevent oxidation of the Nickel cermet electrode material. Air flow to the cell is supplied by the shop air system, after passing through a two-stage extractor/dryer unit. The hydrogen side inlet gas mixture, consisting of hydrogen and nitrogen is mixed with steam by means of a heated humidifier. The dew point temperatures of the nitrogen/hydrogen/steam gas mixture exiting the humidifier and downstream of the cell are monitored continuously using a precision dew point sensors. All gas lines located downstream of the humidifier are heat-traced in order to prevent steam condensation.

The P&ID for button cell testing is similar to Fig. 5 except that an alumina tube is used as a cell holder. The button cells were bonded onto the end of the alumina tube and sealed by glass sealant. The hydrogen/steam electrode is exposed to the hydrogen and steam gas mixture flowing inside the tube, while the air side electrode is exposed to ambient atmospheric air in the furnace. Platinum meshes are attached on both sides of the button cells for current collection.

3. Results and discussion

3.1. MSRI single cells

Two MSRI single cells were tested to investigate the factors that affect their durability. The operating conditions for long-term tests of MSRI cells are listed in Table 1. Gas flow rates of 500 sccm H_2 and 500 sccm N_2 were used on the steam/H_2 side, while 1000 sccm air was used on the air electrode side. The cell operating temperature was 800 °C. Fig. 6 shows the results of the initial performance characterization polarization sweeps of MSRI cell #2 in both the fuel cell and electrolysis modes of operation. The initial voltage–current (*VI*) characteristics for this cell are representative for the MSRI single cells. The *VI* curves in Fig. 6 show the effect of the steam content on cell performance. Curves representing higher steam content show more linear trends both in fuel cell and electrolysis modes. The nonlinearity in the curves at low steam content is associated with the high sensitivity of the Nernst potential to small changes in average steam content. Also, in the electrolysis mode, higher current densities can lead to steam starvation if the average steam content is low. A high inlet dew point temperature, typically 60 °C or higher is suggested for long-term operation in the electrolysis mode [18]. Fig. 6 also shows the dependence of cell area specific resistance (ASR) on current density. The ASR value is calculated based on the following equation:

$$\mathrm{ASR} = (V - V_0)/i$$

where V is the cell operating voltage, V_0 is the open circuit voltage, and i is the current density (A cm^{-2}). The ASR curves are flat at high steam content in both modes, while becoming significantly curved especially in electrolysis mode as steam content decreases. At high steam content, the ASR values are similar in the fuel cell and electrolysis modes. At 80 °C inlet dew point (55.3% steam content), ASR values remain below 0.25 Ω cm^2. Generally, MSRI single cells demonstrate strong initial performance both in the fuel cell and electrolysis modes.

For long-term testing, MSRI cell #1 was initially operated in the fuel cell mode for 120 h, followed by about 300 h of operation in the electrolysis mode. Both modes were controlled galvanostatically at

Table 1
Operating conditions during long-term tests.

Cell, #	Temp, °C	Flow rate, sccm H_2/N_2/air	H_2O content, %
MSRI #1	800	500/500/1000	36.4
MSRI #2	800	500/500/1000	55.3
St. Gobain #1	850	500/500/1000	36.4
St. Gobain #2	850	500/500/1000	55.3
St. Gobain #3	850	500/500/1000	36.4
SOFCPower #1	850	500/500/1000	55.3
Ceramatec #1	850	50/200/0	36.4
Ceramatec #2	850	50/200/0	36.4

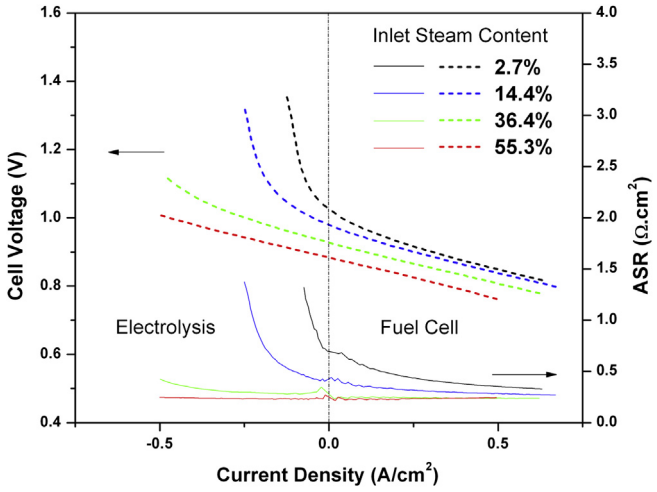

Fig. 6. Polarization curves and calculated ASR values in the fuel cell and electrolysis modes of an MSRI single cell.

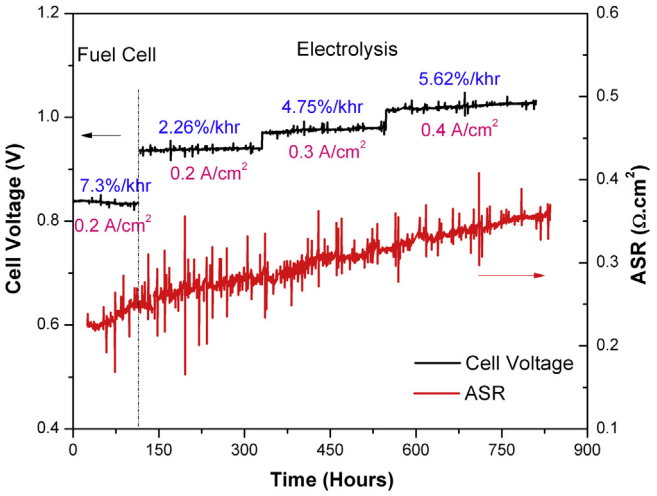

Fig. 8. Long-term test of MSRI #2 in the fuel cell and electrolysis modes. The cell was operated at three different current densities in the electrolysis mode.

0.5 A cm^{-2} in order to compare degradation rates in the two modes. Fig. 7 shows the result of the long-term test of MSRI #1. Cell voltage and ASR are plotted as a function of time. Cell performance was very stable during fuel cell operation with a degradation rate of 0.64% kh^{-1}. After being switched into electrolysis mode, the cell degradation rate increased significantly to 4.26% kh^{-1}. As a comparison, Tietz et al. observed a degradation rate of 3.8% kh^{-1} in a 9000-h test with a current density at 1 A cm^{-2} [22]; we observed 3.2% kh^{-1} degradation rate in MSRI stack tests [23]. However, this degradation rate is still too high for commercial viability.

In order to assess the effect of current density on degradation rate, a different long-term test was performed on MSRI #2. The cell was initially operated in the fuel cell mode for about 110 h, followed by operation in the electrolysis mode over a range of current densities each for about 200 h. The effect of current density on degradation is illustrated in Fig. 8. In the electrolysis mode, degradation rates of 2.26% kh^{-1}, 4.75% kh^{-1} and 5.43% kh^{-1} were observed for current densities of 0.2 A cm^{-2}, 0.3 A cm^{-2}, and 0.4 A cm^{-2}, respectively. These results clearly demonstrate that degradation rate increases as current density increases. Nevertheless, MSRI SOECs still demonstrated excellent overall durability in the electrolysis mode.

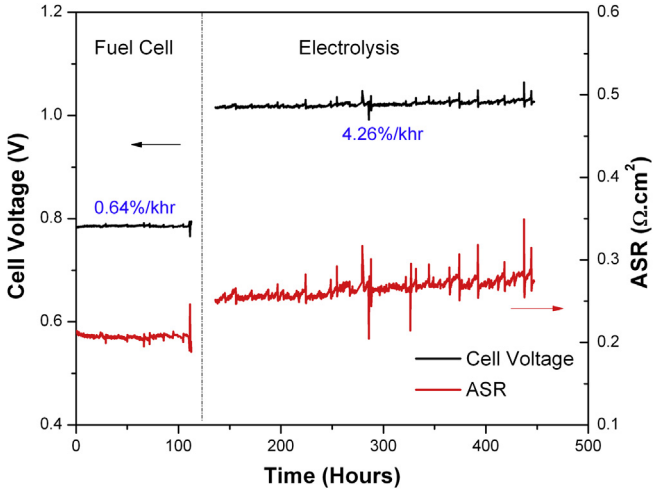

Fig. 7. Long-term test of MSRI #1 in the fuel cell and electrolysis modes.

3.2. Ceramatec button cells

Polarization scans in both fuel cell and electrolysis modes were performed on two Ceramatec button cells. A typical initial performance polarization sweep of a Ceramatec SOEC is shown in Fig. 9. Compared to the electrode-supported SOECs, the electrolyte-supported cells have much higher initial ASR values when they are operated at the same conditions, primarily due to the bulk resistance of the thicker electrolyte (~150 μm compared to ~10 μm). In the case of Ceramatec button cells, the ASR at 70 °C inlet dew point (36.4% steam content) is close to 0.75 Ω cm^2 during polarization sweeps. After the initial *VI* measurements, two Ceramatec button cells were tested only in the electrolysis mode to evaluate the durability of the cells with advanced air electrodes. Ceramatec button cells tested at INL demonstrated exceptional durability during electrolysis.

Ceramatec cell #1 was operated in the electrolysis mode continuously for about 4000 h (5 and 1/2 months) and showed negative degradation (performance increasing) during the entire test. Several power outages occurred during the test and the cell did not survive after a thermal cycle caused by a power outage at

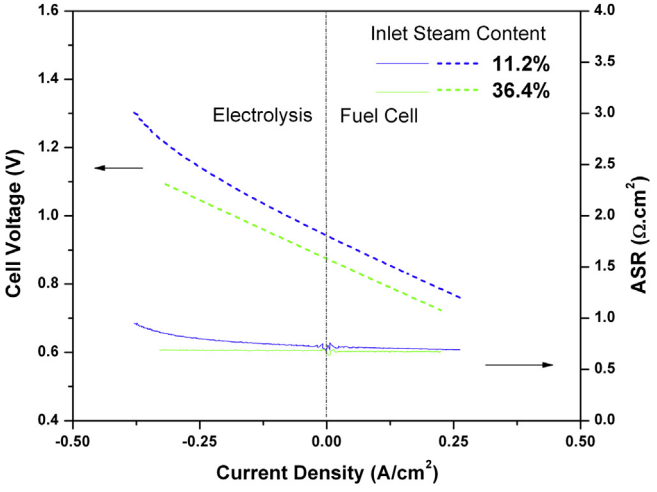

Fig. 9. Polarization curves and calculated ASR values in the fuel cell and electrolysis modes – Ceramatec button cell.

around 4000 h. Fig. 10 represents the results of this long-term test. Due to the limitation of our button cell testing facility, the cell was controlled by constant power supply voltage. Therefore the cell performance improvement is characterized by decrease of the cell voltage but increase of the current density. Periodic adjustments were made in the power supply voltage to maintain a current density close to 0.25 A cm^{-2}. Although not continuously, the cell voltage decreased for 4000 h, while the current density kept increasing. Over this period, the ASR dropped from 2.5 Ω cm^2 to 1.4 Ω cm^2 after. Although the cell performance increased with time during the test, the magnitude of the ASR was still significantly higher than that of the electrode-supported cells. The open-cell voltage was checked regularly during the test (corresponding to the spikes in the voltage data) and found to be steady over the 4000-h operation.

A durability test on Ceramatec cell #2 was conducted afterwards to verify if the performance of Ceramatec cell #1 was repeatable. Fig. 11 shows the results of a long-term durability test of Ceramatec cell #2. The current density was once again maintained at a value close to 0.25 A cm^{-2}. The initial ASR value for this cell was 0.7 Ω cm^2, much lower than the initial ASR value of cell #1. For the first 1100-h operation, cell performance degraded initially and then stabilized at an ASR value of ~1.05 Ω cm^2, which was close to the final ASR value for cell #1. A power outage occurred at around 1100 h, resulting in a sudden increase in ASR. For the following 700 h, the ASR decreased from 1.5 Ω cm^2 to 1.3 Ω cm^2. The cell was shut down finally after another power outage happened at 1850 h. In general, the long-term performance of the two button cells showed distinctly different trends, but the ASR values for the two cells were similar after long-term operation.

The negative degradation (i.e. performance increase) observed on Ceramatec cell #1 is similar to what was found in the stack tests documented in Ref. [23], one of which showed 2% performance increase after initial conditioning. However, the observed performance increase over the long time period cannot be easily explained. More stack and button cell tests will be conducted at INL to fully understand this exceptional behavior.

3.3. St. Gobain single cells

The St. Gobain cells tested at INL were actually developed as SOFCs, based on the Julich technology [24]. Stable performance was expected in the fuel cell mode, while its behavior in the electrolysis mode was unknown. Test results for three St. Gobain single cells with different air electrodes are reported here. Fig. 12 shows the

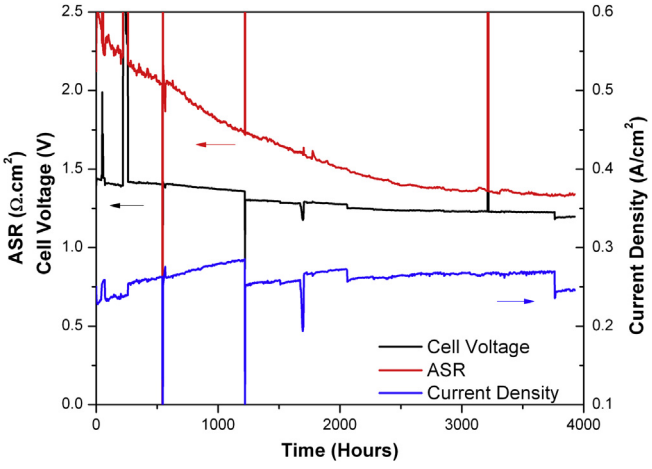

Fig. 10. Long-term electrolysis test of Ceramatec cell #1.

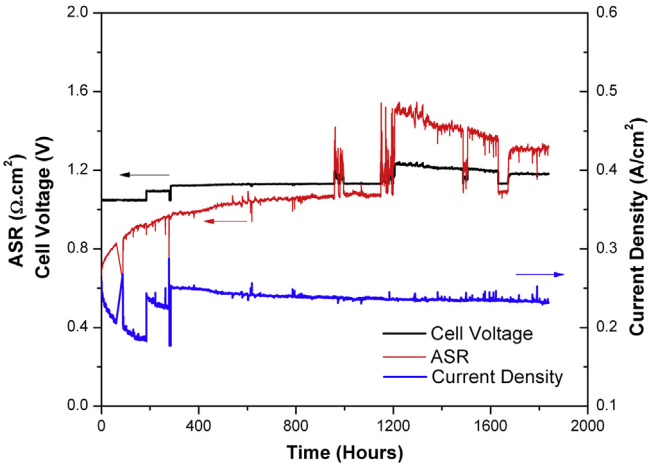

Fig. 11. Long-term electrolysis test of Ceramatec cell #2.

initial polarization sweeps of two single cells; one with modified LSM (black curves) and the other with LSCF (red curves) air electrodes at three different values of steam content. Based on the slopes of the *V–I* curves, the single cell with the LSCF air electrode demonstrated better initial performance than the one with modified LSM electrode.

Following the initial performance evaluation, the single cells were put into long-term operation. Fig. 13 shows the result of a long-term test of St. Gobain cell #1 with modified LSM air electrode. The cell was operated galvanostatically at 0.5 A cm^{-2} at 850 °C with steam content at 36.4%. The cell voltage was very stable in the fuel cell mode with almost zero degradation. However, after switching to the electrolysis mode, the cell exhibited severe degradation immediately. Consequently, the test was shut down after only 5 h operation in the electrolysis mode.

More detailed information on degradation can be obtained from the impedance spectra. Impedance measurements were performed before the tests, after operation in the fuel cell mode, and after 5 h operation in electrolysis mode. Fig. 14 shows the Nyquist plots of the impedance spectra and a post-test photo. The intercept of the

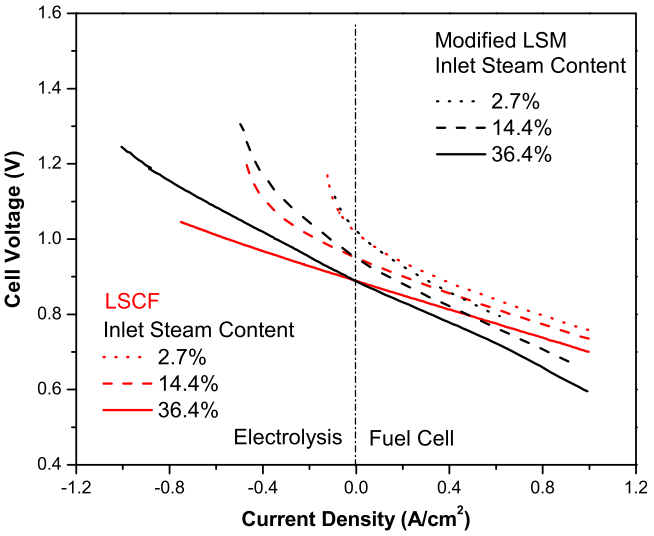

Fig. 12. Polarization curves in the fuel cell and electrolysis modes. Black and red curves show the results of St. Gobain cells with modified LSM and LSCF air electrode, respectively. (For interpretation of the references to colour in this figure legend, the reader is referred to the web version of this article.)

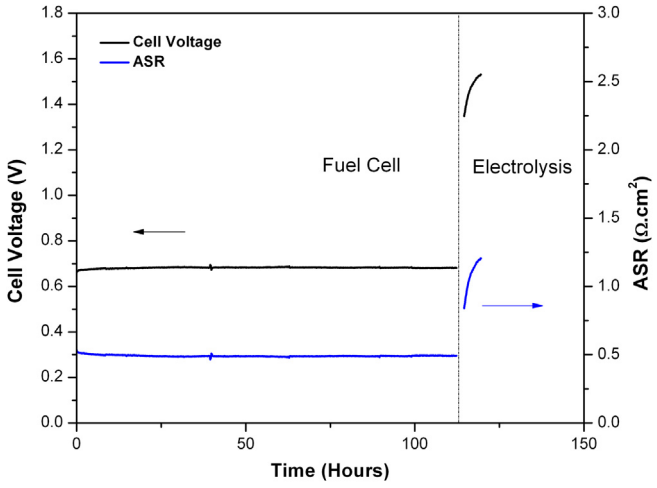

Fig. 13. Long-term test of St. Gobain #1 with modified LSM air electrode. The cell is operated at 0.5 A cm^{-2} at 850 °C.

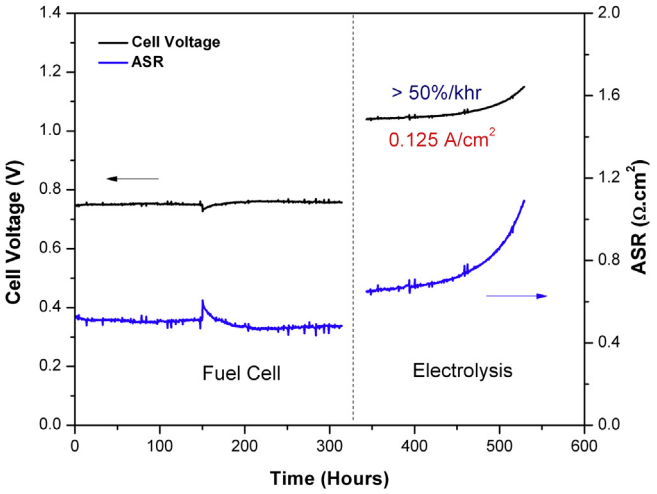

Fig. 15. Long-term test of St. Gobain cell #2 with modified LSM air electrode. The cell was operated at 0.125 A cm^{-2} at 850 °C in the electrolysis mode.

spectra at high frequency with real axis represents the ohmic resistance including electrolyte resistance. It illustrates that the electrolyte remains stable in electrolysis mode. The semi-circles at low frequencies characterize the electrochemical behavior of the electrodes. After operating in electrolysis mode for only 5 h, the shape of semi-circle at low frequencies changed significantly, with a much higher value for the low-frequency intercept, consistent with electrode degradation. Post-test examination revealed that a complete air electrode delamination occurred as is evident in the photo taken after the test. The black air electrode is totally detached from the cell, which is embedded in the cell holder and sealed with white ceramic paste.

The configuration of St. Gobain cell #2 is the same as St. Gobain cell #1. St. Gobain cell #2 was used to investigate cell performance at low current density in the reversible mode. Fig. 15 shows the results of a long-term test of St. Gobain cell #2 with modified LSM air electrode. The cell was operated galvanostatically at 0.125 A cm^{-2} for 550 h at 850 °C with high steam content (55.3%). Again the cell showed no degradation at all in the fuel cell mode, but suffered from severe degradation (more than 50% kh^{-1}) in the electrolysis mode, despite the low current density.

Fig. 16 shows the results of the long-term test of St. Gobain cell #3 with LSCF air electrode. The cell was operated galvanostatically at 0.5 A cm^{-2} at 850 °C with 36.4% steam content. The cell was operated in fuel cell mode for 180 h before switching to electrolysis mode. Significant degradation was again observed in electrolysis mode and the test was shut down after running in electrolysis mode for less than 10 h. Visible delamination of the air electrode was also found in the post-test examination.

3.4. SOFCPower cells

SOFCPower cells were also developed as standard SOFCs. Fig. 17 shows polarization curves representing the initial performance of an SOFCPower cell in both fuel cell and electrolysis modes for four different values of steam content. The cell demonstrated initial performance that was similar to the performance of the MSRI and St. Gobain SOCs. With a thin electrolyte layer, the ASR (~0.5 Ω cm^2) is much lower than that of electrolyte-supported cells. Fig. 18 shows the result of a long-term test of SOFCPower cell #1 with LSCF air

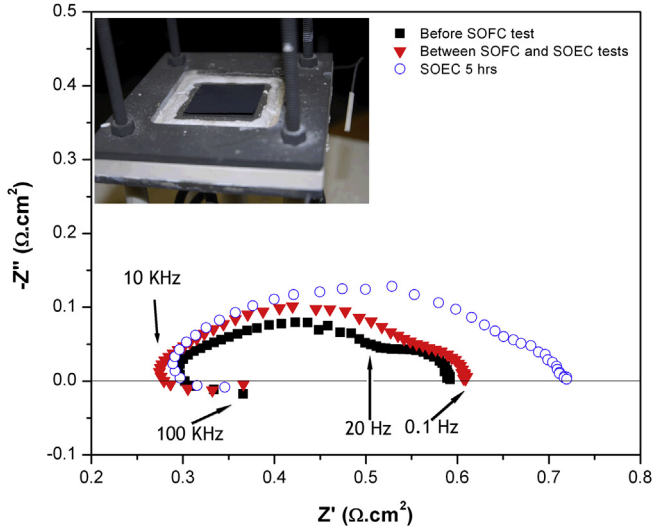

Fig. 14. Nyquist plots of the impedance spectra measured during long-term tests in fuel cell and electrolysis modes at open circuit conditions. The measurements were performed during the test shown in Fig. 13.

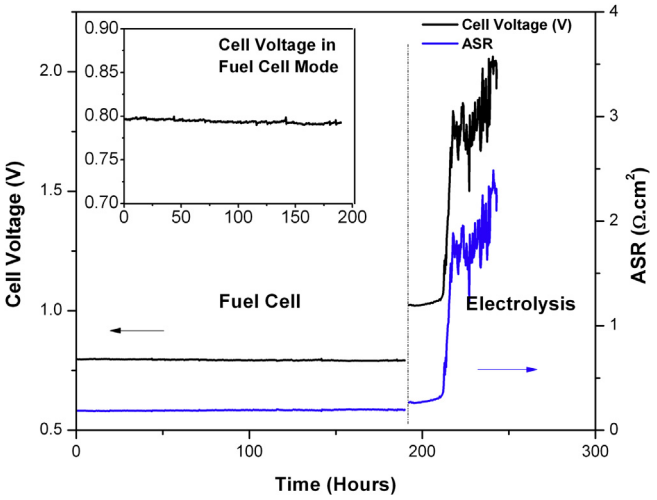

Fig. 16. Long-term test of St. Gobain #3 with LSCF air electrode. The cell was operated at 0.5 A cm^{-2} at 850 °C.

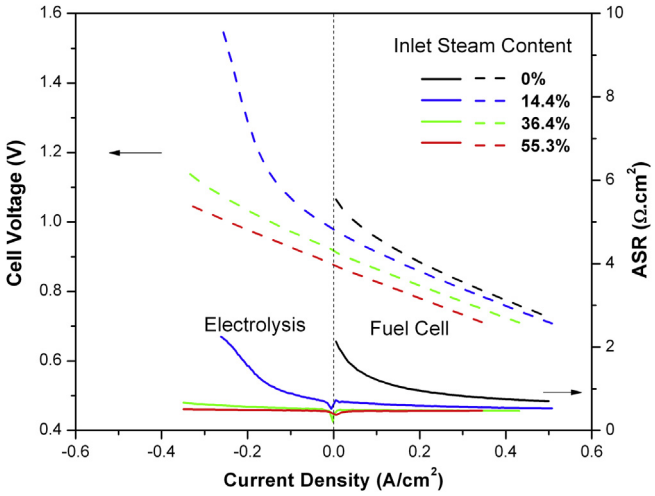

Fig. 17. Polarization curves and calculated ASR values in the fuel cell and electrolysis modes of an SOFCPower SOC.

electrode operating in the reversible mode with a steam content of 55.3%. Initially the cell was operated galvanostatically at 0.175 A cm^{-2} at 800 °C in the fuel cell mode for 230 h. No degradation was found during the fuel cell operation. Actually the performance increased slowly over the first 230 h. The cell was then switched to electrolysis operation with the same current density. Modest degradation was observed after switching to electrolysis mode with a rate of 6.3% kh^{-1} over 200 h. However, after doubling the current density in the electrolysis mode (at 430 h), the degradation rate increased dramatically to more than 100% kh^{-1}. Visible delamination was not found in the post-test examination of this cell.

Note that SOFCPower SOFCs demonstrated better durability than St. Gobain SFOCs. It may due to a ceria-based functional layer used in SOFCPower cells. However, in general, standard SOFCs are not suitable for reversible operation due to their rapid degradation in the electrolysis mode, especially at higher current density. On the other hand, cells that were designed for the SOEC mode, such as MSRI and Ceramatec cells, show acceptable degradation in both the fuel cell and electrolysis mode.

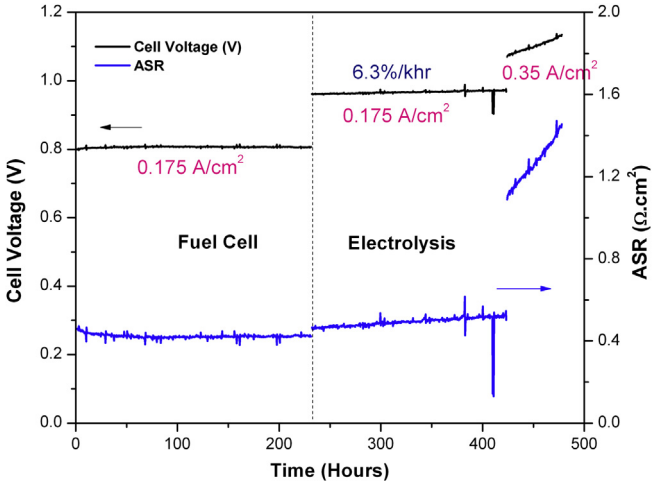

Fig. 18. Long-term test of SOFCPower #1 with LSCF air electrode in the fuel cell and electrolysis modes.

There are several possible mechanisms responsible for degradation in the electrolysis mode in these single-cell tests. Oxygen partial pressure build-up in the electrode–electrolyte interface is a proposed mechanism leading to air electrode delamination [7,19,25,26]. Microstructure coarsening caused by interactions among the material constituents results in a decrease in conductivity and electrochemical activity [8,27]. Seal leakage is another important factor, which can occur during thermal cycles.

4. Conclusion

A newly designed apparatus has been developed for testing of single solid oxide cells in both fuel cell and electrolysis modes of operation. The new apparatus was proved to be robust for multiple experiments. Performance and durability evaluation of SOCs provided by MSRI, Ceramatec, St. Gobain, and SOFCPower in the reversible mode have been performed. MSRI cells demonstrated low degradation rates during durability tests. Test performed at different current densities revealed higher degradation rates at higher current densities. One Ceramatec button cell that was operated for 4000 h in the electrolysis mode showed negative degradation (performance improvement). This exceptional performance was similar to that of one Ceramatec stack tested at INL [23]. The reason for the performance increase remains under further investigation. St. Gobain and SOFCPower single cells showed stable performance in the fuel cell mode, but experienced rapid degradation in the electrolysis mode. These results confirm that cells developed for SOFC applications are not necessarily suitable for the electrolysis mode without modification. More cells will be tested at INL to investigate methods that can further mitigate degradation at the single-cell level.

Acknowledgments

This work was supported by the U.S. Department of Energy, Office of Nuclear Energy, Nuclear Hydrogen Initiative and Next Generation Nuclear Plant Programs under DOE Operations Office Contract DE-AC07-05ID14517. We appreciate the communications from Joseph J. Hartvigsen (Ceramatec), Dr. Greg Tao (MSRI), Dr. Nathalie Petigny (St. Gobain), and Dr. Dario Montinaro (SOFCPower).

References

[1] Markets and Markets, Global Hydrogen Generation Market by Merchant & Captive Type, Distributed & Centralized Generation, Application & Technology – Trends & Forecasts (2011–2016). www.marketsandmarkets.com.
[2] M.A. Laguna-Bercero, Journal of Power Sources 203 (2012) 4–16.
[3] C.M. Stoots, J.E. O'Brien, K. Condie, L. Moore-Mcateer, G. Housley, J.J. Hartvigsen, J.S. Herring, Nuclear Technology 166 (2009) 32–42.
[4] J.E. O'Brien, X. Zhang, G.K. Housley, L. Moore-McAteer, G. Tao, High Temperature Electrolysis 4 kW Experiment Design, Operation, and Results. INL/EXT-12-27082 (Sept. 2012).
[5] A. Hauch, S.H. Jensen, S. Ramousse, M. Mogensen, Journal of the Electrochemical Society 153 (2006) A1741–A1747.
[6] A. Hauch, S.D. Ebbesen, S.H. Jensen, M. Mogensen, Journal of the Electrochemical Society 155 (2008) B1184–B1193.
[7] R. Knibbe, M.L. Traulsen, A. Hauch, S.D. Ebbesen, M. Mogensen, Journal of the Electrochemical Society 157 (2010) B1209–B1217.
[8] V.I. Sharma, B. Yildiz, Journal of the Electrochemical Society 157 (2010) B441–B448.
[9] A. Aguadero, D. Perez-Coll, J.A. Alonso, S.J. Skinner, J. Kilner, Chemistry of Materials 24 (2012) 2655–2663.
[10] S. Elangovan, J.J. Hartvigsen, L.J. Frost, International Journal of Applied Ceramic Technology 4 (2007) 109–118.
[11] F. He, D. Song, R.R. Peng, G.Y. Meng, S.F. Yang, Journal of Power Sources 195 (2010) 3359–3364.
[12] M.A. Laguna-Bercero, J.A. Kilner, S.J. Skinner, Solid State Ionics 192 (2011) 501–504.

[13] O.A. Marina, L.R. Pederson, M.C. Williams, G.W. Coffey, K.D. Meinhardt, C.D. Nguyen, E.C. Thomsen, Journal of the Electrochemical Society 154 (2007) B452–B459.
[14] M. Ni, M.K.H. Leung, D.C. Leung, Journal of Power Sources 163 (2006) 460–466.
[15] M. Ni, M.K.H. Leung, D.Y. Leung, Journal of Power Sources 177 (2008) 369–375.
[16] C.W. Forsberg, Nuclear Technology 166 (2009) 18–26.
[17] G. Haratyk, C.W. Forsberg, Nuclear Technology 178 (2012) 66–82.
[18] J.E. O'Brien, C.M. Stoots, J.S. Herring, J.J. Hartvigsen, Nuclear Technology 158 (2007) 118–131.
[19] J.R. Mawdsley, J.D. Carter, A.J. Kropf, B. Yildiz, V.A. Maroni, International Journal of Hydrogen Energy 34 (2009) 4198–4207.
[20] J.E. O'Brien, C.M. Stoots, J.S. Herring, J. Hartvigsen, Journal of Fuel Cell Science and Technology 3 (2006) 213–219.
[21] C.M. Stoots, J.E. O'Brien, J.S. Hartvigsen, International Journal of Hydrogen Energy 34 (2009) 4208–4215.
[22] F. Tietz, D. Sebolda, A. Brisseb, J. Schefold, Journal of Power Sources 223 (2013) 129–135.
[23] X. Zhang, J.E. O'Brien, R.C. O'Brien, J.J. Hartvigsen, G. Tao, G.K. Housley, International Journal of Hydrogen Energy 38 (1) (2013) 20–28.
[24] R. Steinberger-Wilckens, L. Blum, H.P. Buchkremer, S. Gross, L. de Haart, K. Hilpert, H. Nabielek, W. Quadakkers, U. Reisgen, R.W. Steinbrech, F. Tietz, International Journal of Applied Ceramic Technology 3 (2006) 470–476.
[25] A.V. Virkar, International Journal of Hydrogen Energy 35 (2010) 9527–9543.
[26] K.F. Chen, S.P. Jiang, International Journal of Hydrogen Energy 36 (2011) 10541–10549.
[27] A. Hagen, Y.L. Liu, R. Barfod, P.V. Hendriksen, Journal of the Electrochemical Society 155 (2008) B1047–B1052.